JOURNAL OF GUIDANCE, CONTROL, AND DYNAMICS
Vol. 16, No. 4, July–August 1993

Reaction Wheel Low-Speed Compensation Using a Dither Signal

John B. Stetson Jr.
General Electric Astro Space Division, Princeton, New Jersey 08543

A method for improving low-speed reaction wheel performance on a three-axis controlled spacecraft is presented. The method combines a constant amplitude offset with an unbiased, oscillating dither to harmonically linearize rolling solid friction dynamics. The complete, nonlinear rolling solid friction dynamics using an analytic modification to the experimentally verified Dahl solid friction model were analyzed using the dual-input describing function method to assess the benefits of dither compensation. The modified analytic solid friction model was experimentally verified with a small dc servomotor actuated reaction wheel assembly. Using dither compensation abrupt static friction disturbances are eliminated and near linear behavior through zero rate can be achieved. Simulated vehicle response to a wheel rate reversal shows that when the dither and offset compensation is used, elastic modes are not significantly excited, and the uncompensated attitude error reduces by 34:1.

Nomenclature

C_1 = offset signal, N-m
C_2 = dither signal amplitude, N-m
D = wheel bearing viscous friction coefficient, N-m-s/rad
J = reaction wheel inertia, kg-m^2
T_c = motor actuated wheel command torque, N-m
T_r = vehicle reaction torque, N-m
T_v = wheel bearing viscous friction torque, N-m
X = reaction wheel state vector, $[\dot{x}, y]$
$\dot{x}$ = reaction wheel angular rate, rad/s
y = solid friction torque, N-m
α = smoothing parameter
β_1 = bearing rest slope parameter, (N-m-rad)$^{-1}$
β_2 = coulomb friction, N-m
γ = dither signal frequency, rad/s
λ = solid friction natural frequency, rad/s
ϕ_1 = analytic signum function
ϕ_2 = bearing friction-slope function

Introduction

WHEN a reaction wheel approaches zero rate, the bearing viscous friction effect is small, and rolling solid friction dominates the relationship between commanded and actual vehicle control torque. An existing method compensates for the solid friction discontinuity at zero rate by adding an offset to the torque command signal that has a constant amplitude approximating the coulomb (velocity independent) friction, and with the sign of the wheel rate. Although this method improves performance, its usefulness is restricted by the traditional incorrect assumption that coulomb friction with a signum function of wheel rate accurately models the complete solid friction dynamics. Furthermore, when the wheel is required to provide smooth, bidirectional control with a nominal zero rate (if the vehicle is required to hold an inertial reference, for example), the offset method fails completely, and vehicle attitude control degrades. Another method attempts to suppress the zero-rate solid friction discontinuity by using high gain wheel rate feedback summed with the torque command. This method improves performance somewhat, but its applicability is limited by low on-orbit power availability and limit-cycle oscillations that appear as soon as the gain is increased to a level where performance improvement is noticeable.

The best choice for a friction compensation system therefore must be asymptotically stable, must use the least possible power, and must provide the most linear behavior through zero rate.

The method presented here combines a constant amplitude offset with an unbiased, oscillating dither to harmonically linearize the stiff, rolling solid friction dynamics. The constant offset term corrects for coulomb friction at nonzero wheel rate, and the dither signal, applied only when the wheel rate is low to save power, alters the abrupt rate reversal static friction characteristic to a pseudolinear viscous friction term. The resulting closed-loop attitude control performance with a wheel rate reversal correspondingly improves. The maximum

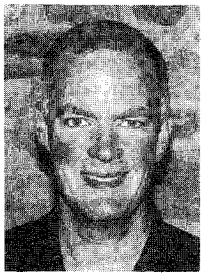

John B. Stetson Jr. works for the Martin Marietta Astro Space Division Control and Dynamics Analysis Group in Princeton, New Jersey. He received his B.S. in Mechanical Engineering from Swarthmore College and is pursuing the M.S.E. and Ph.D. degrees in Mechanical Engineering and Applied Mathematics at Temple University in Philadelphia, Pennsylvania. His research interests are in precision actuator design and nonlinear mechanics and he holds several U.S. patents in these fields. Currently he leads Guidance and Navigation Design for the Air Force DMSP and NOAA TIROS satellite systems.

Received Feb. 19, 1991; revision received Aug. 3, 1992; accepted for publication Aug. 6, 1992.

attitude error induced by a wheel rate reversal decreases to one-thirty-fourth its uncompensated value and to one-half the value when only offset compensation is used.

Reaction Wheel Analytical Model

Dahl has derived and experimentally verified a mathematical model for solid friction between two rigid bodies.[2] In the case of rolling motion such as that between a bearing ball and its adjacent races, resistive friction is characterized by brittle elastic behavior. For small displacements about its rest position, the system exhibits a linear stress-strain relationship. However, when the internal cohesive bond stresses at the leading and trailing bearing-race interface exceed a value equivalent to the coulomb force, continuous bond rupture and rolling motion occur.[3]

Figure 1 shows the reaction wheel mathematical block diagram for the special case of rolling solid friction dynamics. The solid friction torque y is a function of the wheel rate $\dot{x}$, the sign of the wheel rate $\Phi_1(\dot{x})$, and the experimentally determined friction-slope function $\Phi_2(\dot{x})$. In the original derivation, the function $\Phi_1(\dot{x})$ was defined as the signum function of wheel speed. To formulate the equations of motion as a continuous matrix state equation for analysis, $\Phi_1(\dot{x})$ must be differentiable so an analytic approximation to the signum function is required. Junkins et al.[4] determined that the parametric hyperbolic tangent function most simply and accurately approximates the signum function for small α:

$$\operatorname{sgn}(\dot{x}) \approx \tanh\left(\frac{\dot{x}}{1-\alpha}\right) \tag{1}$$

where $0 \le \alpha \le 1$ is a smoothing parameter. A comparison of the experimental and simulated results using this function for $\Phi_1(\dot{x})$ showed good agreement for $0.88 \le \alpha$. With this substitution, the equations of motion corresponding to Fig. 1 can be formulated as a second-order time invariant nonlinear state equation:

$$\dot{X} = F(X) \tag{2}$$

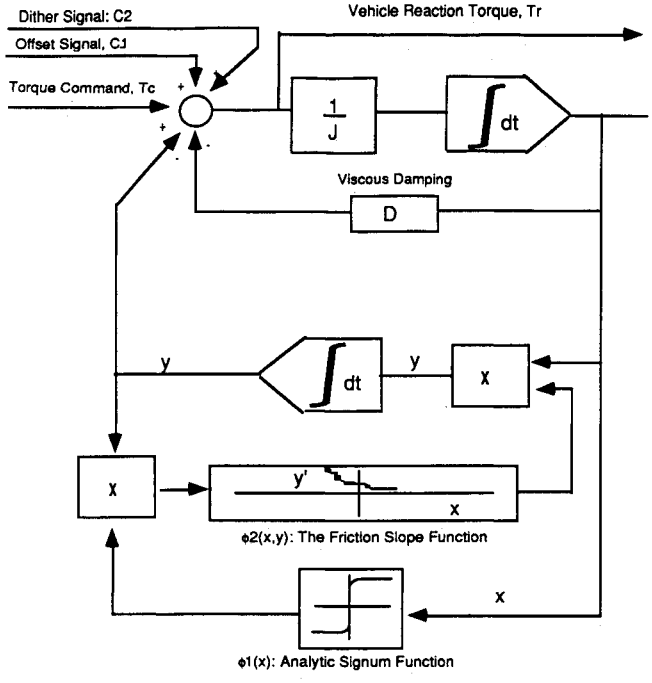

Fig. 1 Reaction wheel dynamics.

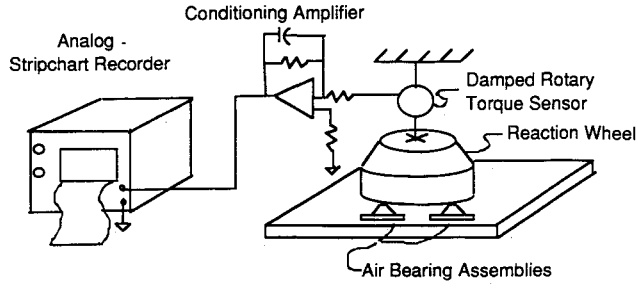

Fig. 2 Reaction wheel experimental apparatus.

Table 1 General Electric small reaction wheel solid friction parameters[a]

Power stage type	Phased current source
Actuator motor type	dc brushless
Rotor inertia, J, kg-m^2	0.0430
Viscous friction coefficient, D, N-m-s/rad	0.009
Bearing rest slope parameter, β_1, (N-m-rad)$^{-1}$	12,200
Coulomb friction, β_2, N-m	0.014
Digital speed resolution, rpm	1.46 (12 bits magnitude, 1 bit sign)
Maximum speed, rpm	±6000

[a]Parameters were measured with two identical bearings rotating in unison.

where the state vector $X = [\dot{x}\ y]^T \ni X \in R^2$. Then Eq. (2) becomes

$$\begin{bmatrix}\ddot{x}\\ \dot{y}\end{bmatrix} = \begin{bmatrix} -J^{-1}(y + D\dot{x} + T_a) \\ \dot{x}y\phi_1(\dot{x})\phi_2(\dot{x}, y)\end{bmatrix} = \begin{bmatrix} -J^{-1}(y + D\dot{x} + T_a) \\ \beta_1\dot{x}[y \cdot \tanh(\dot{x}/1-\alpha) - \beta_2]^2\end{bmatrix} \tag{3}$$

where parameters β_1 and β_2 can be experimentally determined for a specified bearing assembly. The homogeneous solution of Eq. (3) ($\dot{X} = 0$) yields the single equilibrium condition

$$\dot{x} = y = 0 \tag{4}$$

This condition corresponds to the wheel at rest with no internal cohesive bond strain and therefore no resistive friction torque. To insure that Eq. (4) satisfies physical intuition as a stable (Lyapunov) equilibrium, the equations of motion are linearized about Eq. (4) yielding the linear time invariant form

$$\dot{X} = AX + BU \tag{5}$$

where the matrix A is the Jacobian of Eq. (2) evaluated at Eq. (4). Performing the necessary algebra yields

$$A = \begin{bmatrix} -J^{-1}D & -J^{-1} \\ \beta_1(-\beta_2)^2 & 0\end{bmatrix}, \quad B = \begin{bmatrix} J^{-1} \\ 0\end{bmatrix} \tag{6}$$

The characteristic equation for matrix A yields two eigenvalues

$$\lambda^2 + \frac{D}{J}\lambda + J^{-1}\beta_1(-\beta_2)^2 = 0 \ \therefore\ \lambda_{1,2} = \frac{-J^{-1}D}{2} \pm \frac{\sqrt{(J^{-1}D)^2 - 4J^{-1}\beta_1(-\beta_2)^2}}{2} \tag{7}$$

For typical reaction wheel bearing systems, the viscous damping $J^{-1}D$ is smaller than the solid friction restoring force term $J^{-1}\beta_1(-\beta_2)^2$ and so the system eigenvalues are complex con-

jugate pairs with negative real parts. Therefore, as the wheel comes to rest, it experiences the damped, oscillatory motion about zero rate identified by Dahl[2] and Staph.[5]

Experimental Model Verification

Precision laboratory measurements of a General Electric 0.14 N-m capacity reaction wheel were made to validate the theoretically predicted solid friction behavior for a complete reaction wheel assembly. Figure 2 shows a schematic of the wheel and its air-bearing support structure. A precision torque sensor fixed to the wheel and the support structure measures vehicle reaction torque directly. The wheel rotor is supported by two identical 17-mm-diam class 7 precision ball bearings both having a 266 N preload. Because of precise alignment, the bearings move in unison and can be considered to act as a single bearing for analysis purposes. The measured wheel parameters used in the simulation are given in Table 1.

Substituting the Table 1 values into Eq. (7), the eigenvalues describing the motion near zero rate are $\lambda_{1,2} = -0.1 \pm j7.45$ rad/s.

Figures 3a and 3b show measured and simulated reaction torque time histories as the wheel coasts to rest. Allowing for the identified 4 Hz test rig natural frequency, a 7.2 rad/s damped natural frequency is easily identified. Although there is excellent agreement between the measured and simulated natural frequency, the actual wheel motion decays in 8 s whereas the linearized eigenvalues suggest that a longer 33 s time is needed. Staph[5] presents results for a similar reaction wheel showing motion decay in about 10 s. Harris[3] speculates that a laminar dissipation mechanism proportional to the rate squared is present when bearing displacements are small. This effect causes more rapid damping than the linear analysis predicts without significantly changing the natural frequency.

Solid Friction Harmonic Linearization Using Dither

Boyer[6] discovered that the steady, nonlinear oscillations near zero output voltage exhibited in A-class linear amplifiers could be eliminated by adding a small, unbiased sinusoidal "dither" signal to the amplifier input. Furthermore, if the dither signal frequency was chosen sufficiently higher than the input signal frequency, the amplified input was not affected. This phenomenon is explained by applying the dual input describing function technique for signals of widely different frequencies.[1] When two signals of widely different frequencies are summed together, the frequency separation of the two components allows the magnitude of the low frequency wave to be assumed constant over any one period of the high frequency wave with little error. Thus, applying the combined signal to a nonlinear element linearizes the input/average output characteristic. In addition, if the nonlinear element has a time integrating property, the output will be linearly related to the low frequency input component.[1]

Consider adding such a dither signal C_2 to the reaction wheel torque command (Fig. 1) when the wheel rate is near zero. If the dither frequency γ is much greater than the solid friction dynamics natural frequency [Im (λ1, λ2)], the torque feedback path can be considered open.[1] Additionally, since the wheel's speed is near zero, the viscous term may be neglected, and the vehicle reaction torque may then be written as the sum of commanded and dither torques

$$T_r(t) = T_c + C_2\sin(\gamma t) \tag{8}$$

The reaction wheel speed (the input to the nonlinear solid friction dynamics) is proportional to the time integral of the reaction torque

$$\dot{x}(t) = J^{-1}\int [T_c + C_2\sin(\gamma t)]\mathrm{d}t \tag{9}$$

Again, since the dither frequency is high relative to the commanded torque frequency, T_c can be assumed constant over one period of the dither signal. With this assumption, carrying out the integration for one period of the dither signal yields

$$\dot{x}(t) = J^{-1}[T_c t + (C_2/\gamma)\cos(\gamma t)] \tag{10}$$

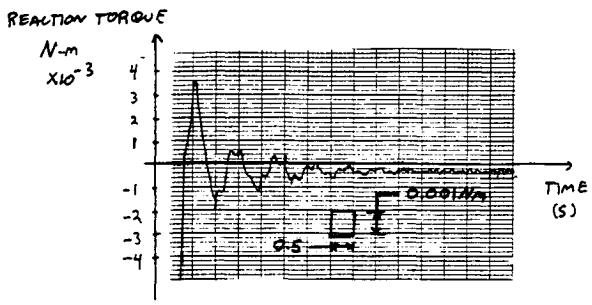

Fig. 3a Measured wheel stop reaction torque.

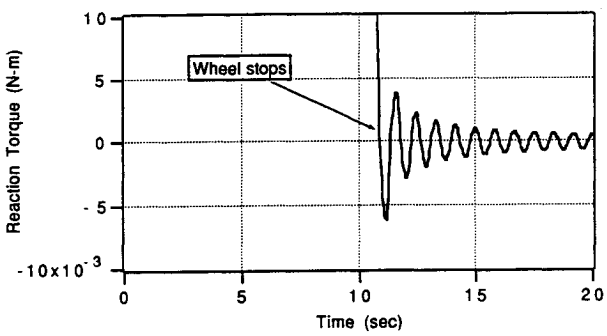

Fig. 3b Simulated wheel stop reaction torque.

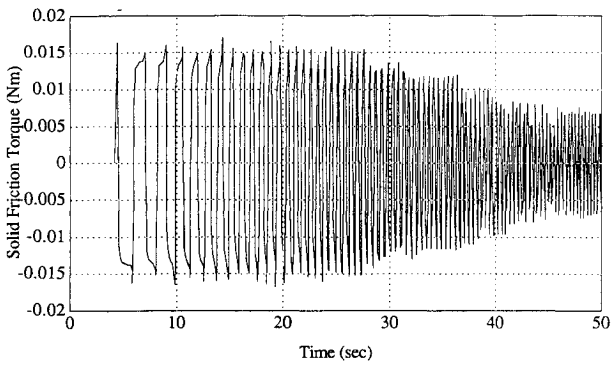

Fig. 4a Dithered solid friction torque time history.

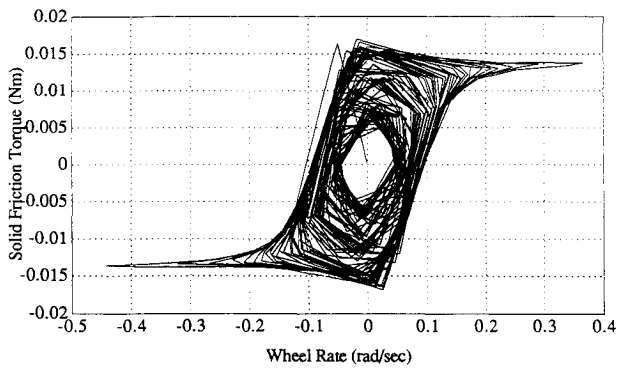

Fig. 4b Dithered solid friction torque characteristic.

Table 2 General Electric space vehicle parameters used in the simulation

Parameter	Value	Units
x-axis inertia	4616	kg-m^2
y-axis inertia	2626	kg-m^2
z-axis inertia	3155	kg-m^2
Dominant mode fixed base frequency	1.2	rad/s
Dominant mode natural frequency	0.25	rad/s
Modal coupling coefficients (x, y, z)	34.9, 10.0, 2.4	$\sqrt{\text{kg-m}^2}$
Dominant mode damping ratio	0.002	
Orbit rate	0.001059	rad/s

The dither signal C_2 produces only zero-mean wheel motion and since γ is large, the motion amplitude is small. The commanded torque causes an incremental change in wheel speed as expected, and its net effect on the wheel (and vehicle) position are unchanged by the dither's presence. In addition, any significant vehicle structural oscillations are unlikely since the dither is applied only for short durations (typically less than 10 s) when a wheel is near zero rate.

The wheel rate is the input to the solid friction nonlinearity. Because the modified solid friction model satisfies the describing function applicability constraints,[6] i.e., it is time invariant, it does not generate subharmonics of the input signal, and it has a time integrating property, the solid friction y can be written as a linear combination of the input frequencies $\dot{x}$

$$y = a_0 + b_1\sin(\gamma t) + a_1\cos(\gamma t) + \cdots + \text{higher harmonics} \quad (11)$$

where

$$a_0 = \frac{\gamma}{\pi}\int_{\pi/\gamma}^{\pi/\gamma} \dot{x}(t)\,dt, \qquad a_1 = \int_{\pi/\gamma}^{\pi/\gamma} \dot{x}(t)\cos(n\gamma t)\,dt$$

$$b_1 = \int_{\pi/\gamma}^{\pi/\gamma} \dot{x}(t)\sin(n\gamma t)\,dt \quad (12)$$

The effective solid friction torque is the average output amplitude a_0

$$\bar{y} = a_0 \quad (13)$$

Instead of calculating a_0 analytically, the solid friction torque vs wheel rate trajectory was simulated for the reaction wheel described in Table 1.

A 0.014 N-m amplitude dither signal ($C_2 = \beta_2$) was used. The dither frequency was initially applied at low frequency ($\gamma = 0.25$ rad/s) to demonstrate the friction characteristic for typical on-orbit wheel behavior without compensation. Then, γ was increased linearly (as a sine sweep function) to three times the solid friction system natural frequency, or 22 rad/s.

Figure 4a shows the applied dither torque vs time, and Fig. 4b shows the solid friction torque vs wheel rate. At low frequency, the torque/rate characteristic shows predominant relay-like behavior associated with pure coulomb friction. At nonzero rates, the torque approaches the ± 0.014 N-m coulomb value listed in Table 1. The hysteresis indicates internal bearing cohesive forces attempting to arrest wheel motion. Significant linearization occurs when γ is increased. At higher frequency, even with C_2 unchanged, the abrupt torque reversal characteristic near zero rate is replaced by a smooth elliptical trajectory less than one-half the coulomb torque amplitude. This behavior motivates dither frequency selection to be above the solid friction natural frequency to provide greater vehicle motion isolation and increased linearization.

Addition of the constant offset term C_1 equal to β_2 with the sign of $\dot{x}$ (see Fig. 1) completes the dither-offset compensation system for typical on-orbit reaction wheel control. The offset corrects the vehicle reaction torque to compensate for the coulomb torque component, and the dither aids passage through zero rate.

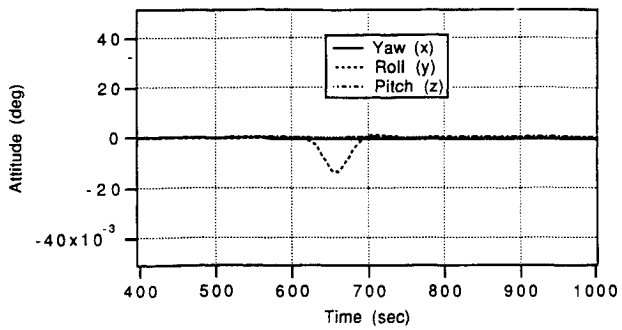

Fig. 5a Vehicle attitude for an uncompensated wheel reversal.

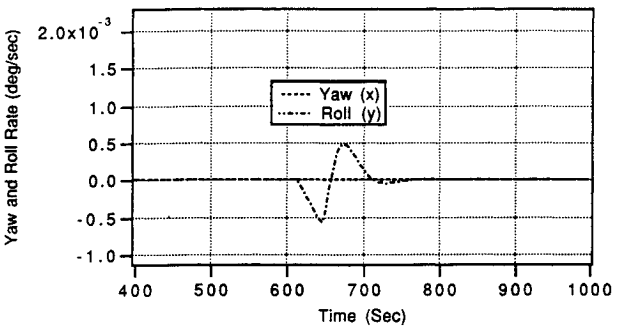

Fig. 5b Vehicle rate for an uncompensated wheel reversal.

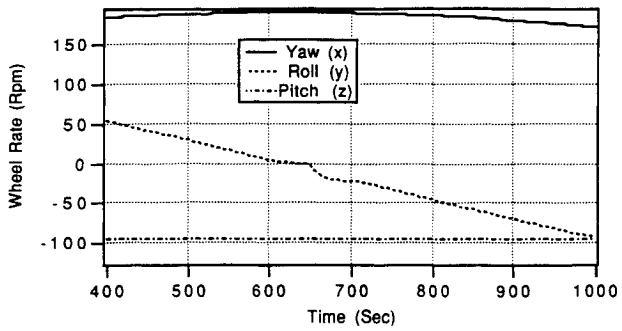

Fig. 5c Vehicle wheel speeds for an uncompensated wheel reversal.

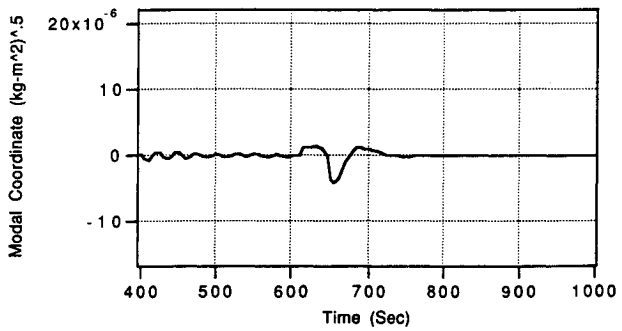

Fig. 5d Dominant vehicle modal displacement for an uncompensated wheel reversal.

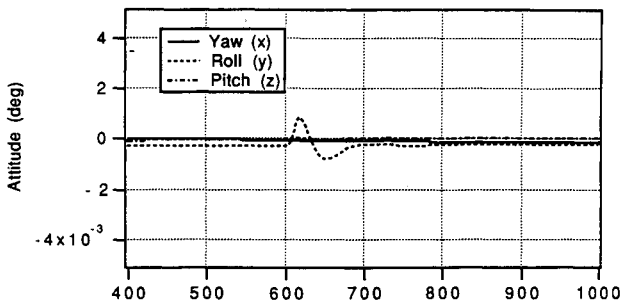

Fig. 6a Vehicle attitude using offset compensation.

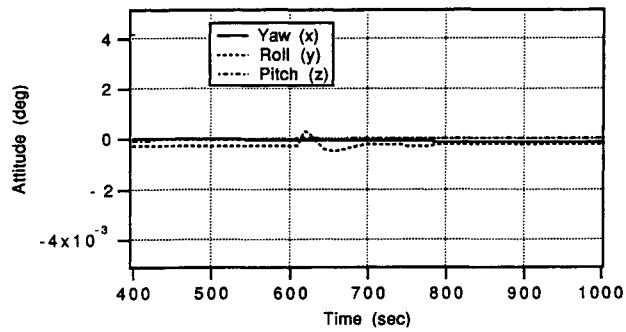

Fig. 7a Vehicle attitude using offset and dither compensation.

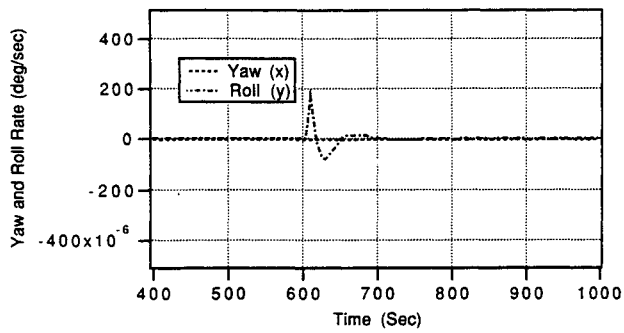

Fig. 6b Vehicle rate using offset compensation.

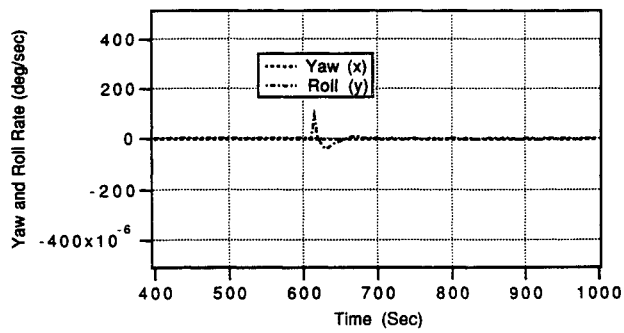

Fig. 7b Vehicle rate using offset and dither compensation.

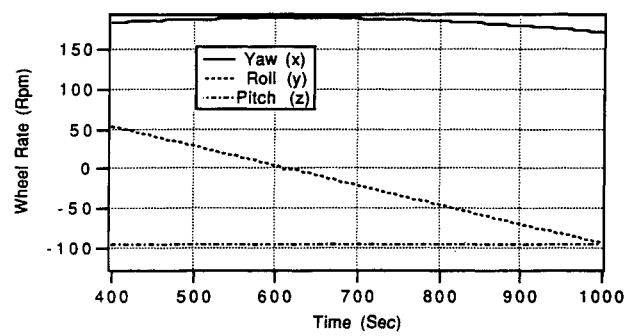

Fig. 6c Vehicle wheel speeds using offset compensation.

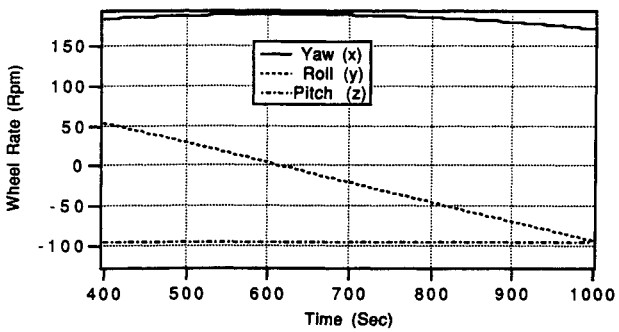

Fig. 7c Vehicle wheel speeds using offset and dither compensation.

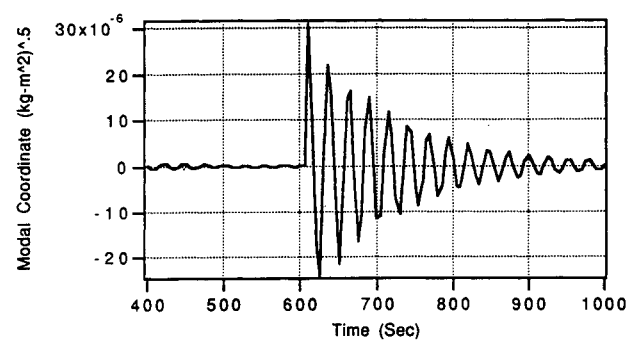

Fig. 6d Dominant vehicle modal displacement using offset compensation.

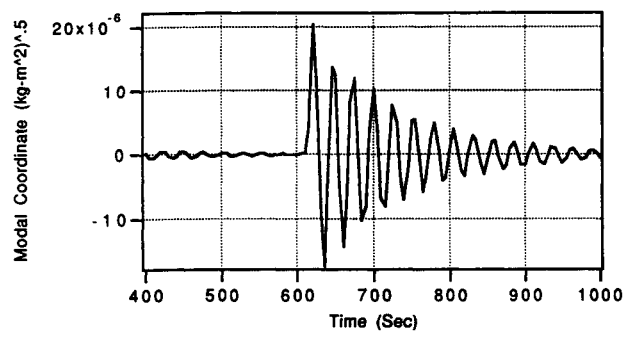

Fig. 7d Dominant vehicle modal displacement using offset and dither compensation.

Spacecraft Attitude Error Reduction

The reaction wheel dynamics including the experimentally verified solid friction model were incorporated into a general, nonlinear space vehicle time simulation program to evaluate vehicle attitude performance using dither and offset compensation. The vehicle characteristics are typical of a precision meteorological observation platform with a maximum of 0.01 deg (36 arc-s) allocated for attitude control errors per axis. The simulation includes the effects of rigid and flexible vehicle attitude dynamics with sensor and control system zero-mean band limited white noise, quantization, and sampling. The General Electric vehicle mass and structural properties used in the simulation are listed in Table 2. The vehicle is nominally Earth oriented with its yaw x axis facing the Earth, its roll y axis aft, and its pitch z axis along the positive orbit normal. The dominant appendage flexibility is represented by a scalar modal coordinate that corresponds to the motion of the vehicle's solar array first linear mode. A unity amplitude modal coordinate motion ($\sqrt{\text{kg-m}^2}$) approximately corresponds to one-twenty-fifth of the roll y axis rate (rad/s). This hybrid coordinate, substructure synthesis realization is described by Likins[7] and is used extensively throughout the industry.

Figures 5a–5d show simulated vehicle attitude, rate, wheel rate, and modal coordinate displacement time histories when the roll y axis reaction wheel passes through zero rate at 620 s. The vehicle was initialized at orbit rate with no attitude errors and with 200 rpm on the yaw and roll reaction wheels. About 1/8 orbit later (625 s), the roll wheel approaches zero rate. The solid friction arrests the wheel for approximately 30 s (Fig. 5c) as the control torque builds up enough to exceed the coulomb friction at the opposite wheel rate. During this time, the vehicle coasts out of control, and the roll error (Fig. 5a) builds up to a maximum 0.017 deg (61 arc-s) before the wheel breaks loose and control is restored. This error not only violates the required 0.01 deg allocation, but persists for more than 75 s as the control system removes the error. Since the dominant wheel crossing disturbance torque spectral components are at a very low frequency, the 0.25 rad/s structural oscillation (Fig. 5d) is weakly excited by the wheel crossing but disappears shortly after wheel motion is restored.

The vehicle simulation was repeated using offset compensation alone, and the results are shown in Figs. 6a–6d. As with the wheel dynamics simulation, a ± 0.15 rad/s threshold was chosen to represent a 12 bit magnitude, 1 bit polarity digital tachometer resolving the wheel's full 6000 rpm range (Table 1). For clarity, one least significant bit is $6000/4095 = 1.47$ rpm $= 0.15$ rad/s. This simulation best demonstrates that coulomb friction is only a portion of the total solid friction. Even though the 0.014 Nm offset amplitude was chosen to perfectly cancel the coulomb friction ($C_1 = -\beta_2$), and the offset was applied when the wheel speed was within 0.15 rad/s from zero rate, the solid friction again stops the wheel rotation for about 10 s, and a 0.001 deg roll error (Fig. 6a) occurs. Therefore, if offset compensation alone is to be used effectively, an offset amplitude somewhat greater than the coulomb friction level must be applied to "force" the wheel through zero rate. Although this procedure is often done in practice, it is difficult to select how much the offset amplitude should exceed the coulomb friction level: too much offset produces an opposite attitude error of the same magnitude as with too little offset. In addition, the solid friction characteristics near zero rate have been observed to change with time,[2] making periodic offset level software changes necessary. The disturbance resulting from imperfect cancellation causes significant structural excitation (Fig. 6d) that couples to the vehicle rate (Fig. 6b). Although the attitude error reduction from the uncompensated condition is dramatic, the 3.6 arc-s still occupies a significant portion of the overall error budget.

When a 0.014 N-m amplitude ($C_2 = \beta_2$), 22 rad/s (three times the wheel's solid friction natural frequency) dither is added to the coulomb offset compensation and simulated, the maximum vehicle error decreases from 0.001 deg using offset alone to 0.0005 deg. Figures 7a–7d show the vehicle attitude, rate, wheel rate, and modal coordinate displacement time histories. The dither is applied with the offset when the wheel is within 0.15 rad/s of zero speed. The dither prevents the solid friction from arresting wheel motion (Fig. 7c) resulting in a smooth passage through zero rate. In this case, the wheel was stopped for only 2 s. A corresponding 2:1 attitude error reduction over offset compensation alone results from this improvement (Fig. 7a). The structural excitation amplitude (Fig. 7d) is also reduced because the abrupt, step discontinuity induced by imperfect offset compensation is reduced by the dither signal.

Conclusion

The work presented here shows that the addition of a simple, zero-mean periodic dither signal to the reaction wheel command signal linearizes the abrupt coulomb friction effect as the wheel passes through zero rate. The dither amplitude should be no greater than twice the coulomb friction level and the dither frequency should be three to five times the rest oscillation frequency. Using a dither amplitude equal to twice the coulomb friction level and a dither frequency equal to three times the wheel's solid friction natural frequency, the uncompensated vehicle attitude error reduced by 34:1. The dither compensation improves coulomb friction compensation attitude errors by 2:1. Structural motion excited by abrupt, imperfect coulomb friction offset compensation is reduced by the dither's linearizing effect. The dither and offset signals can be generated by either the spacecraft flight computer or a small special purpose analog circuit accompanying the reacting wheel control electronics. If the dither logic is implemented in a practical sampled data spacecraft flight computer, the dither frequency will be limited to typical control frequencies ranging from 2 to 5 Hz. Although this frequency is sufficient for most reaction wheels, some wheels may require that the dither signal be created using an analog implementation to obtain better performance.

References

[1]Gibson, J. E., *Nonlinear Automatic Control*, 1st ed., McGraw-Hill, New York, 1963, Secs. 9.2 and 9.9.

[2]Dahl, P. R., "A Solid Friction Model," The Aerospace Corp., TOR-158 (3107-18), El Segundo, CA, May 12, 1968.

[3]Harris, T. A., *Rolling Bearing Analysis*, 2nd ed., Wiley, New York, 1984, Sec. 13.3.

[4]Junkins, J. L., Byers, R., and Vadali, S., "Near-Minimum Time Closed Loop Slewing of Flexible Spacecraft," *Journal of Guidance, Control, and Dynamics*, Vol. 13, No. 1, 1990, pp. 57–65.

[5]Staph, R., "Torque Irregularities in Reaction Wheels," *Proceedings of the 2nd European Space Mechanisms & Tribology Symposium* (Meersburg, Germany), Oct. 9–12, 1985, pp. 127–131.

[6]Boyer, R. C., "Sinusoidal Signal Stabilization," M.S. Thesis, Purdue Univ., West Lafayette, IN, Jan. 1960.

[7]Likins, P. W., "Results of Flexible Spacecraft Attitude Control Studies Using Hybrid Coordinates," *Journal of Spacecraft and Rockets*, Vol. 8, No. 3, 1971, pp. 264–272.